Journal of
Applied Crystallography
ISSN 0021-8898

Received 14 August 2006
Accepted 1 February 2007

Small-angle fibre diffraction studies of corneal matrix structure: a depth-profiled investigation of the human eye-bank cornea

Andrew J. Quantock,[a]* Craig Boote,[a] Robert D. Young,[a] Sally Hayes,[a] Hidetoshi Tanioka,[b] Satoshi Kawasaki,[b] Noboru Ohta,[c] Tohko Iida,[c] Naoto Yagi,[c] Shigeru Kinoshita[b] and Keith M. Meek[a]

[a]Structural Biophysics Group, School of Optometry and Vision Sciences, Cardiff University, Cathays Park, Cardiff CF10 3NB, UK, [b]Department of Ophthalmology, Kyoto Prefectural University of Medicine, Kyoto 602, Japan, and [c]Japan Synchrotron Radiation Research Institute, Spring-8, Hyogo, 679-5198, Japan. Correspondence e-mail: quantockaj@cf.ac.uk

In the cornea of the eye light transmission is facilitated by the regular arrangement and uniform diameter of collagen fibrils that constitute the bulk of the extracellular corneal matrix. Matrix architecture, in turn, is believed to be governed by interactions between collagen fibrils and proteoglycan molecules modified with sulfated glycosaminoglycan side chains. Here, we outline the contribution made by small-angle X-ray scattering studies of the cornea in understanding the role of sulfated glycosaminoglycans in the control of collagen architecture in cornea, and present new depth-profiled microbeam data from swollen human eye-bank corneas that indicate no significant change in collagen fibril diameter throughout the tissue, but a lower collagen interfibrillar spacing in the anterior-most stromal regions compared with the ultrastructure of the deeper cornea.

1. Introduction

The cornea of the eye is a unique, optically clear connective tissue. Its transparency, however, does not arise from it being a homogeneous material with a constant refractive index as was originally thought, but rather is based on interference effects between light scattered by the tissue's main non-specular light scattering elements, collagen fibrils (Maurice, 1957; Hart & Farrell, 1969; Benedek, 1971; Farrell, 1994). These fibrils are uniformly about 300 Å in diameter, and are organized into a stacked lamellar array that forms a composite structure approximately 500 µm thick in man (Komai & Ushiki, 1991). This collagenous portion of the cornea – called the corneal stroma – constitutes 90% of its thickness, and is bound on distal and proximal sides, respectively, by epithelial and endothelial cell layers. Collagen fibrils in the corneal stroma, because they are arranged with a degree of spatial order, give rise to an interfibrillar reflection on small-angle X-ray scattering (SAXS) patterns (Goodfellow *et al.*, 1978). In the years since the first synchrotron X-ray diffraction patterns were obtained from (bovine) cornea using the DESY facility (Meek *et al.*, 1981), this approach has become an established tool for structural investigations of the corneal stroma. In this article, we first review recent applications of SAXS to the study of corneal ultrastructure in developing chicks and transgenic mice, with a focus on the role of sulfated proteoglycans in the control of corneal biosynthesis and homeostasis. We then present new microbeam SAXS data which shed light on collagen fibrillar alignment, spacing and diameter as a function of depth in the human eye-bank cornea.

1.1. Developmental events

Knowledge of how the corneal stroma is formed during embryogenesis is important to help understand some fundamentals of corneal matrix biology, and also to better appreciate wound healing in the adult situation because this recapitulates some developmental events. The established model for the study of corneal development is the chicken eye, in which corneal morphogenesis is dominated by well documented structural transformations that govern tissue form and function (Linsenmayer *et al.*, 1998). Light and electron microscopy have revealed that from embryonic day 12 to hatch at day 21 a condensation takes place during which time the tissue thins and the collagen fibrillar array becomes remodelled (Birk & Trelstad, 1984; Linsenmayer *et al.*, 1990; Hirsch *et al.*, 1999). Also, around this time the cornea becomes transparent, with early spectrophotometry measurements showing that at developmental day 14 only about 40% of incident white light is transmitted, whereas by day 18 transmission is over 90%, close to adult levels (Coulombre & Coulombre, 1958). SAXS patterns from cornea are the product of the square of the scattering amplitude for a single cylinder, F^2, an interference function $G(K)$, plus background scattering from non-collagenous components and non-fibrillar collagens. Patterns thus contain information that allows us to calculate average diameter of collagen fibrils in the cornea as well as their mean centre-to-centre Bragg spacing. We have used this approach to study the spatial and temporal alterations in the collagen fibril array during chick corneal development and the onset of tissue transparency. Initial experiments conducted on station X12B at the NSLS, Brookhaven National Laboratory, disclosed that collagen interfibrillar spacing as an average throughout the whole thickness of the cornea became significantly reduced during the developmental day 12 to day 18 time period (Quantock *et al.*, 1998). Subsequent investigations on station 2.1 at the SRS, Daresbury Laboratory, using a beam focused to 1 mm × 0.5 mm at the specimen and a 9 m camera, have further indicated that collagen interfibrillar

Bragg spacing drops in a two-stage fashion during day 12–18 matrix compaction. Thus, from day 12 onwards regions of the stroma with a relatively high water content become dehydrated. Some days later, at the day 16–17 timepoint, a more homogeneous compaction of collagen fibrils takes place (Siegler & Quantock, 2002).

In the extrafibrillar corneal matrix of a number of species, proteoglycan macromolecules of the keratan sulfate and/or chondroitin sulfate/dermatan sulfate varieties are believed to govern collagen fibrillar architecture (Borcherding *et al.*, 1975). Biochemical work (Cornuet *et al.*, 1994) has indicated that the sulfated form of keratan sulfate accumulates in the embryonic chick cornea over approximately the same timescale as the tissue becomes transparent, suggestive of a functional role in collagen arrangement. Our current research is now developing immunochemical assays of corneas that have been studied using SAXS to investigate how matrix changes correspond to changes in the amount of sulfated proteoglycans in the cornea.

1.2. Transgenic studies

As mentioned, proteoglycans in the corneal stroma are believed to influence corneal matrix architecture, and to do so *via* associations with collagen. These molecules are composed of a repeat disaccharide glycosaminoglycan side chain(s) linked to a core protein. Keratan sulfate is the major glycosaminoglycan in cornea, and can be linked to one of three core proteins, lumican, keratocan or mimecan. Lumican and keratocan are related proteoglycans, with lumican known to have a regulatory influence over the expression of keratocan at the transcriptional level (Carlson *et al.*, 2005). In recent years, the production of gene-targeted mice with proteoglycan null mutations has facilitated research into the respective and combined functions of these molecules in the control of extracellular matrix morphogenesis (Chakravarti, 2002; Kao & Liu, 2002). To better understand the role of keratan sulfate proteoglycans in cornea we undertook a series of SAXS experiments on the corneas of mature gene-targeted mice with homozygous deletions of lumican, keratocan or mimecan. This work indicated that the collagen fibrillar matrix was significantly altered in the lumican-null mutant (Quantock *et al.*, 2001), and that the changes occurred concurrently with a loss of corneal transparency (Chakravarti *et al.*, 1998). SAXS data from the corneas of neonatal mice at the time of eye opening (day 10–12) showed that the transient thickening of the corneal stroma that occurs at that time (Song *et al.*, 2003) is not likely to be due to a homogeneous and widespread change in the collagen interfibrillar spacing, but rather a cellular or localized swelling (Beecher *et al.*, 2006). This analysis further suggested that the structural defects in collagen organization caused by a lumican deficiency which we see in the adult mouse are not defects that arise *de novo* with age, but stem from early postnatal events (Beecher *et al.*, 2006). Alterations of collagen fibrillar structure in the keratocan-deficient cornea are more subtle than those in the lumican-deficient cornea (Meek, Quantock *et al.*, 2003), and do not result in any appreciable loss of corneal transparency (Liu *et al.*, 2003). SAXS measurements of matrix architecture in the optically clear corneas of the mimecan-null mouse detected no significant differences in collagen interfibrillar spacing, diameter or level of local order in the fibrillar array (Beecher *et al.*, 2005). Thus, despite the fact that mouse cornea contains keratan sulfate which is relatively undersulfated when compared with other species (Young *et al.*, 2005), the molecules do influence the formation and maintenance of a structurally normal corneal stroma. Recent attempts involving SAXS to uncouple the roles of the whole proteoglycan from its sulfated glycosaminoglycan side chain(s) have pointed to a functional role for the sulfotransferase enzyme that adds sulfate groups to keratan sulfate (Hayashida *et al.*, 2006).

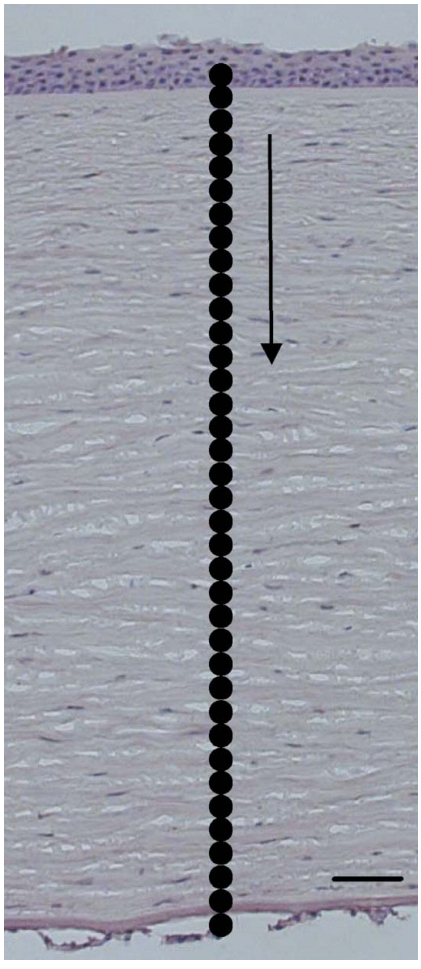

Figure 1
A full thickness histological section through the left cornea investigated here, with the positions at which the 25 µm diameter microbeam was passed represented as black dots. The cornea was scanned with the microbeam in an anterior-to-posterior direction as indicated by the arrow. Bar = 75 µm.

1.3. Human cornea

SAXS experiments have been used to measure collagen fibrillar architecture in the human corneal stroma in a number of pathologic conditions, often involving proteoglycan deficiencies [for a review of these experiments see Meek & Quantock (2001)]. The approach has also documented collagen ultrastructure (spacing and diameter) in human corneas as a function of the position across the cornea at a spatial resolution of 0.4–1.0 mm, comparing central and peripheral tissue (Boote *et al.*, 2003), and on dehydration to levels below physiological (Fratzl & Daxer, 1993). These data were collected with the X-ray beam directed parallel to the optical axis and passing through the whole thickness of the isolated cornea. This gives good representative data on collagen fibrillar ultrastructure and orientation as an average throughout the whole stromal thickness, but cannot provide data on any structural differences which may occur throughout the cornea at different depths. Microscopic observations of human corneas have indicated that collagen fibrillar and lamellar arrangements in anterior and posterior tissue regions are structurally distinct (Komai & Ushiki, 1991; Freund *et al.*, 1995; Radner *et al.*,

1998). Thus, to investigate corneal ultrastructure in a depth-profiled manner we obtained SAXS patterns from human eye-bank corneas using a 25 μm microbeam passed through corneal strips in a direction parallel to the plane of the cornea.

2. Experimental and analytical procedures

A left-right pair of human corneas, approximately 8 mm in diameter, was provided for research purposes with full informed consent and institutional approval by the Northwest Lions Eye Bank, Seattle, USA. On receipt in the Department of Ophthalmology, Kyoto Prefectural University of Medicine, the corneas had been immersed in culture media for 4 d and were swollen as a result. Each cornea was bisected across its diameter, and one half immersed in OCT compound (RM Lamb Ltd, Eastbourne, UK) for examination (7 μm-cryosections stained with haematoxylin) by light microscopy.

From the flat edges of the remaining two half-corneas, two thin strips (estimated at 400 μm thick) were dissected freehand with ophthalmic surgical tools. These were immediately placed between two pieces of clingfilm to limit dehydration, frozen at 253 K and transported on dry ice to SPring-8 for examination using SAXS. All experiments were conducted on beamline 40XU using an X-ray beam (λ = 0.83 Å) with a circular area measuring 25 μm diameter at the specimen. At the beamline the strips of cornea were allowed to thaw and, still wrapped in clingfilm, were secured onto a Mylar sheet and mounted in the path of the beam in a horizontal orientation with the cut edge perpendicular to the incident beam direction. A series of sequential 0.2 s exposures was then obtained at 25 μm steps vertically through the centre of the specimen, traversing its entire thickness (Fig. 1). SAXS patterns were recorded on a cooled CCD camera (ORCAII-ER, Hamamatsu Photonics) coupled with an X-ray image intensifier (V5445P, Hamamatsu Photonics) 3 m behind the specimen. Data analysis was carried out in accordance with protocols described in Quantock *et al.*, 2001, with the position of the first-order equatorial reflection (*i.e.* the interference function) used to calculate the mean centre-to-centre collagen fibril Bragg spacing. The first subsidiary maximum of the experimental data, which arises from the fibril transform, was used to ascertain average fibril diameter (Meek & Quantock, 2001). Calibration was achieved using the meridional reflections from hydrated rat-tail tendon, which index on 670 Å.

After data collection the corneal strip from the left cornea was immersed overnight in 2% glutaraldehyde in a 0.1 *M* phosphate buffer for examination by transmission electron microscopy. The next day it was washed three times in buffer and stored in fresh buffer for 10 d until further processing. At that time the strip was dissected into one central and two peripheral segments which were post-fixed in 1% osmium tetroxide for 1 h, then contrasted en bloc in 0.5% aqueous uranyl acetate for a further 1 h. The tissue was then dehydrated by immersion in 70%, 90%, and twice 100% ethanol each for 15 min. After immersion in propylene oxide for 30 min specimens were infiltrated with Araldite resin which was cured in an oven at 333 K for 48 h. Ultra-thin sections were prepared on a Leica EMUC6 ultra-microtome using a diamond knife and collected on uncoated G300 mesh copper grids. They were subsequently examined in a Philips 208 transmission electron microscope after staining with saturated aqueous uranyl acetate and lead citrate.

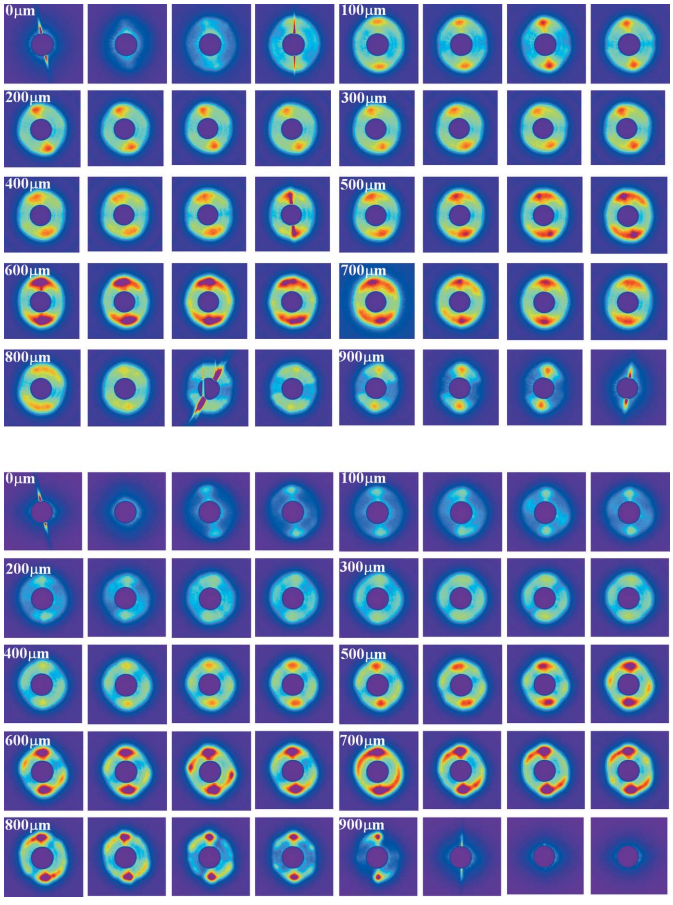

Figure 2
A series of SAXS patterns representing scans in 25 μm steps across the whole depth of left (top montage) and right (bottom montage) human eye-bank corneas. Reflections from deeper tissue regions are more intense with occasional satellite reflections. Equatorial and meridional directions are vertical and horizontal, respectively.

3. Results and discussion

As initially demonstrated by Goodfellow and colleagues (1978) using a laboratory-based X-ray generator, SAXS patterns from the cornea possess a first-order equatorial (*i.e.* collagen interfibrillar) reflection that arises due to the regular arrangement of stromal collagen fibrils. From such patterns and using synchrotron radiation with the X-ray beam passed through the isolated cornea in a direction perpendicular to the plane of the cornea along what would have been the optical axis in the intact eye, the average centre-to-centre collagen inter-fibrillar Bragg spacing in human cornea has been measured at around 500–550 Å (Gyi *et al.*, 1988; Boote *et al.*, 2003). Early experiments on bovine cornea showed that if an X-ray beam was passed through the edge of a strip of cornea in a direction perpendicular to the optical axis (*i.e.* parallel to the plane of the cornea), then a SAXS pattern was produced in which the axial collagen reflections appeared on the meridian with the interfibrillar reflection on the equator (Sayers *et al.*, 1982). Now, with the advent of microfocus technology we are in a position to pass a microbeam through the edge of a cornea at different depths – as shown in Fig. 1 – and obtain diffraction patterns from localized tissue regions to investigate collagen fibrillar and lamellar organization.

Microbeam SAXS data collected in a depth-dependent fashion from human eye-bank corneas as indicated in Fig. 1 are presented in Fig. 2 as a series of consecutive diffraction patterns representing a linear scan across the tissues. Successive patterns across a left-right pair of human eye-bank corneas were obtained at 25 μm steps with a 25 μm diameter microbeam so that the whole thickness of each

cornea was scanned and sampled. Previous work has shown that in the anterior stroma, collagen lamellae measured by electron microscopy in human eye-bank eyes are between 0.2 μm and 1.2 μm thick, whilst in the posterior stroma they are up to 2.5 μm thick (Komai & Ushiki, 1991). Thus, as a rough assessment each SAXS pattern presented here is estimated to be formed by X-ray scattering from between 20 and 40 lamellae, with more and thinner lamellae likely sampled in superficial tissue regions. Each scan with the 25 μm microbeam was started and finished beyond the edge of the tissue, and based on whether or not a SAXS pattern was formed (and assuming no epithelial or endothelial contribution to the patterns in the regions of interest) data are indicative of left and right corneal stromas that are, respectively, 925 μm and 850 μm thick. In the physiologic situation the human cornea is between 500 μm and 550 μm thick, with the swelling in the tissues examined here being typical of eye-bank corneas preserved for transplantation as a result of storage in culture medium.

SAXS patterns from the superficial 200 μm or so of both corneas examined consist of an interfibrillar reflection on the equator indicating that collagen fibrils/lamellae align mostly parallel to the corneal surface (Fig. 2). Previous light and electron microscopic studies of the human cornea have shown that collagen lamellae in the anterior stroma are more branched and interwoven than those in deeper tissue regions (Polack, 1961; Radner *et al.*, 1998), with fibrils and lamellae running obliquely, at unstated angles, to the corneal surface (Komai & Ushiki, 1991). This is evident from transmission electron microscopy of the anterior left cornea studied here (Fig. 3). The current SAXS patterns (Fig. 2) disclose that collagen fibrils in this interwoven, anterior low-swelling zone have an average spread of alignments that extends over approximately 20° of arc (*i.e.* approximately ±10° either side of the plane of the cornea). Beneath the anterior 200 μm or so of stroma, interfibrillar reflections become progressively broader circumferentially. This is indicative of a greater spread of collagen alignments around the plane of the cornea, with the appearance of occasional satellite reflections suggestive of subpopulations of fibrils/lamellae subtending fairly large angles with the plane of the cornea. These features are particularly evident in the deeper two-thirds of the stroma, and we contend are a result of the stroma swelling in a direction perpendicular to the tissue plane and the separation of interwoven lamellae that this brings about. An interesting feature is that the interfibrillar reflection in the posterior stroma is confined to the equator, pointing to lamellae that run parallel to the corneal surface.

It is clear that with increasing depth SAXS patterns become progressively more intense (Fig. 2), though at present we have no definitive explanation as to why this is so. Tissue dissections were made freehand, thus we cannot rule out the possibility that the deep cornea might have been proportionally thicker in the path of the X-ray beam. Conceivably this would lead to more intense scattering from the posterior cornea, but we consider it unlikely to be a major cause of the increased posterior scattering seen in these experiments because dissections were made carefully and any thickness variation would be fairly minimal. Structural differences do exist in cornea between anterior and posterior regions of the stroma, and these might underlie the more intense SAXS patterns from deep tissue apparent here. For example, in bovine cornea a greater differential in the refractive index mismatch between collagen fibrils and extrafibrillar material exists in the deeper stroma (Meek, Leonard *et al.*, 2003). Perhaps, a greater electron density mismatch may exist also, which might contribute to the more intense SAXS patterns posteriorly.

X-ray intensity scans across the SAXS patterns (Fig. 4) show an interference function arising from the fairly regular arrangement and spacing of collagen fibrils in the cornea, and a fibril transform approximated as scattering from single cylinders. Calibration of the system with the 670 Å collagen repeat from rat-tail tendon allows us to calculate values for the mean centre-to-centre collagen interfibrillar Bragg spacing and average collagen fibril diameter (Fig. 5). Within the resolution of the system collagen fibril diameter appears to change little across the depth of the stroma, averaging 35.4 nm ± 0.3 nm and 35.2 nm ± 0.4 nm (mean ± SD) in left and right corneas, respectively. These values are close to previous SAXS measurements of fibril diameter as an average throughout the whole thickness of the

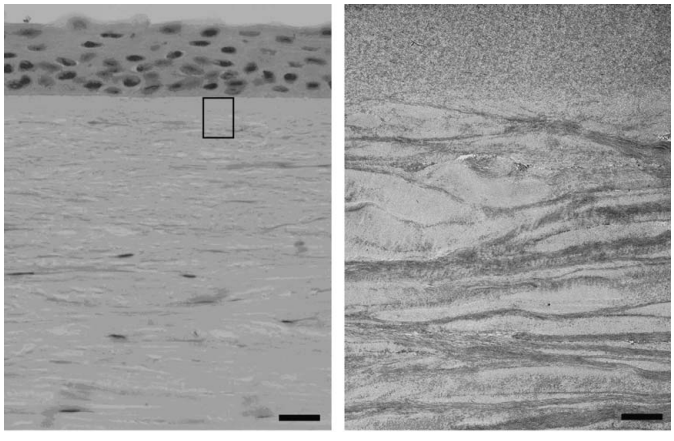

Figure 3
Morphology of anterior stroma in the left cornea from which SAXS patterns were obtained. A histological section (left), stained with haematoxylin, shows epithelial cells at the top with underlying Bowman's layer and stromal lamellae running horizontally. Bar = 30 μm. The box indicates a representative location of the region shown by electron microscopy (right). Bowman's layer is a homogeneous meshwork of collagen fibrils (top), overlying the superficial collagenous lamellae which branch and interweave. Bar = 5 μm.

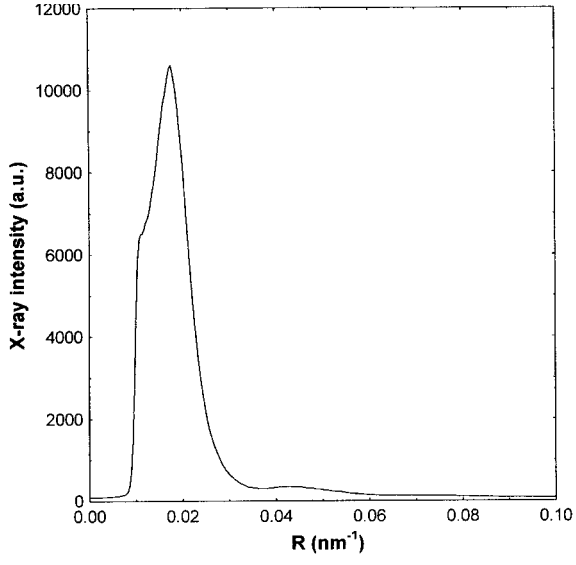

Figure 4
Vertical scan across a representative SAXS pattern from the centre outwards with the interference function clearly visible at around R = 0.018 nm^{-1}, and the fibril transform at around R = 0.045 nm^{-1}. The reciprocal spacing, R, is equivalent to $Q/2\pi$, where $Q = (4\pi/\lambda)\sin\theta$. The wavelength of the X-ray beam, λ, is 0.83 Å and θ is measured as half the scattering angle between the incident and diffracted beam.

human cornea when the cornea has become swollen *in vitro* (Boote *et al.*, 2003) and when it has become oedematous *in situ* because of corneal endothelial dysfunction (Quantock *et al.*, 1991). The lack of significant collagen fibril swelling with increased corneal hydration is in line with previous *in vitro* SAXS/WAXS (wide-angle) investigations into the swelling behaviour of isolated bovine cornea, which showed that with elevated levels of corneal hydration water preferentially distributes in the extrafibrillar matrix rather than within fibrils (Meek *et al.*, 1991). Collagen interfibrillar Bragg spacing in the swollen human eye-bank cornea does seem to exhibit some depth-dependence, with collagen fibrils in the anterior 200 µm or so of the tissue being more closely spaced (Fig. 5). Representative electron microscopical images of collagen fibrils perhaps show a more close fibril spacing in the anterior, compared to mid, stroma (Fig. 6). However, this is fairly difficult to discern, illustrating the value of quantitative SAXS data in ultrastructural investigations of the cornea.

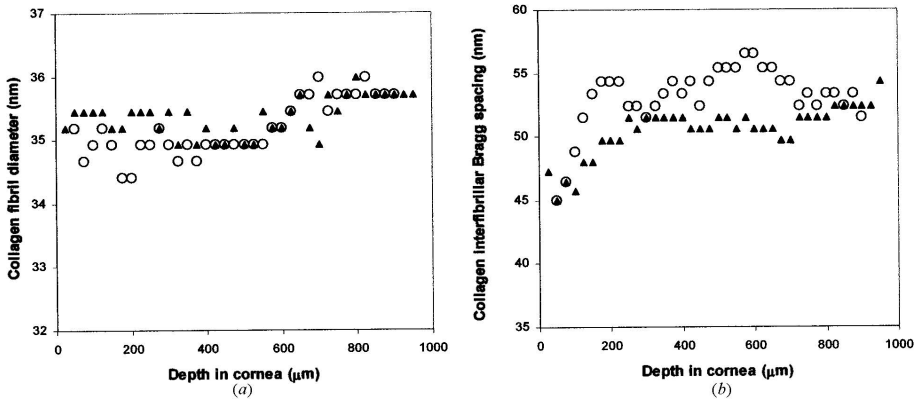

Figure 5
Average collagen fibril diameter and mean centre-to-centre collagen fibril Bragg spacing in the left (solid triangles) and right (open circles) human eye-bank corneas. In the anterior regions of both corneas a lower fibril spacing is apparent.

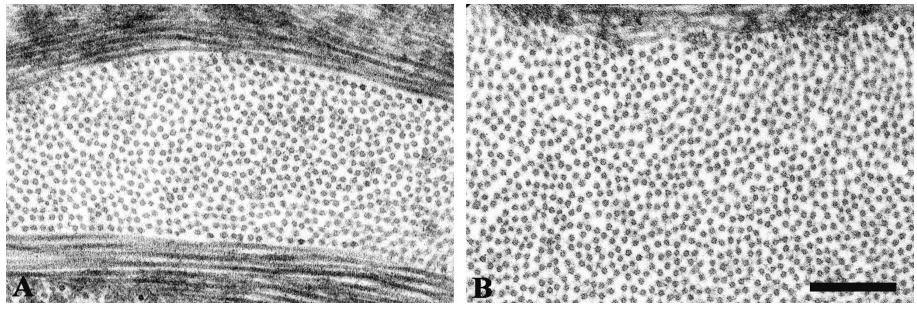

Figure 6
High-magnification cross-sectional images of collagen fibrils within individual lamellae of the swollen left eye-bank cornea in (A) a region of the anterior-most stroma within 50 µm of the corneal surface, and (B) the mid stroma at a depth of 400–500 µm. Bar = 300 nm.

Restricted tissue swelling in the anterior human eye-bank cornea is in line with the finding that even in human corneas maximally swollen to about 1400 µm by immersion in deionized water, the anterior-most 100–120 µm of the stroma does not swell, a property that has been attributed to the tightly interwoven lamellar architecture of the superficial stroma (Muller *et al.*, 2001). The proteoglycan composition of the corneal stroma in a number of species is known to vary with tissue depth (Castoro *et al.*, 1988; Bettelheim & Plessy, 1975), which leads us to consider that it is the variable content and regulatory influence of these molecules throughout the human cornea that might contribute to differences in fibril organization, specifically closer fibril packing which we have here documented in the anterior stroma of the swollen human eye-bank cornea. Subsequent experiments will apply a similar microbeam approach to studies of the human cornea maintained close to physiologic hydration.

The work described in this article was supported by the BBSRC, MRC, EPSRC, NIH, CCLRC and JASRI. Thanks to K. Quantock for help with production of figures. The experiment at SPring-8 was performed with the support of the BBSRC and Sasakawa Foundation, and under approval of SPring-8 Program Review Committee (2006A1012).

References

Beecher, N., Carlson, C., Allen, B. R., Kipchumba, R., Conrad, G. W., Meek, K. M. & Quantock, A. J. (2005). *Invest. Ophthalmol. Vis. Sci.* **46**, 4046–4050.
Beecher, N., Chakravarti, S., Joyce, S., Meek, K. M. & Quantock, A. J. (2006). *Invest. Ophthalmol. Vis. Sci.* **47**, 146–150.
Benedek, G. B. (1971). *Appl. Opt.* **10**, 459–473.
Bettelheim, F. A. & Plessy, B. (1975). *Biochem. Biophys. Acta*, **381**, 203.
Birk, D. E. & Trelstad, R. L. (1984). *J. Cell Biol.* **99**, 2024–2033.
Boote, C., Dennis, S., Newton, R. H., Puri, H. & Meek, K. M. (2003). *Invest. Ophthalmol. Vis. Sci.* **44**, 2941–2948.
Borcherding, M. S., Blacik, L. J., Sittig, R. A., Bizzell, J. U., Breen, M. & Weinstein, H. G. (1975). *Exp. Eye Res.* **21**, 59–70.
Carlson, E. C., Liu, C. Y., Chikama, T. I., Hayashi, Y., Kao, C. W. C., Birk, D. E., Funderburgh, J. L., Jester, J. V. & Kao, W. W. Y. (2005). *J. Biol. Chem.* **280**, 25541–25547.
Castoro, J. A., Bettelheim, A. A. & Bettelheim, F. A. (1988). *Invest. Ophthalmol. Vis. Sci.* **29**, 963–968.
Chakravarti, S. (2002). *Glycoconj. J.* **19**, 287–293.
Chakravarti, S., Magnuson, T., Lass, J. H., Jepsen, K. J., LaMantia, C. & Carroll, H. (1998). *J. Cell Biol.* **141**, 1277–1286.
Cornuet, P. K., Blochberger, T. C. & Hassell, J. R. (1994). *Invest. Ophthalmol. Vis. Sci.* **35**, 870–877.
Coulombre, A. J. & Coulombre, J. L. (1958). *J. Cell. Comp. Physiol.* **51**, 1–11.
Farrell, R. A. (1994). *Principles and Practice of Ophthalmology*, edited by D. M. Albert & S. A. Jacobiec. Philadelphia: Saunders.
Fratzl, P. & Daxer, A. (1993). *Biophys. J.* **64**, 1210–1214.
Freund, D. E., McCally, R. L., Farrell, R. A., Cristol, S. M., L'Hernault, N. L. & Edelhauser, H. F. (1995). *Invest. Ophthalmol. Vis. Sci.* **36**, 1508–1523.
Goodfellow, J. M., Elliott, G. F. & Woolgar, A. E. (1978). *J. Mol. Biol.* **119**, 237–252.
Gyi, T. J., Meek, K. M. & Elliott, G.F. (1988). *Int. J. Biol. Macromol.* **10**, 265–269.
Hart, R. W. & Farrell, R. A. (1969). *J. Opt. Soc. Am.* **59**, 766–774.
Hayashida, Y., Akama, T. O., Beecher, N., Lewis, P., Young, R. D., Meek, K. M., Kerr, B., Hughes, C. E., Caterson, B., Tanigami, A., Nakayama, J., Fukada, M. N., Tano, Y., Nishida, K. & Quantock, A. J. (2006). *Proc. Natl Acad. Sci. USA*, **103**, 13333–13338.
Hirsch, M., Noske, W., Prenant, G. & Renard, G. (1999). *Exp. Eye Res.* **69**, 267–277.
Kao, W. W. Y. & Liu, C. Y. (2002). *Glycoconj. J.* **19**, 275–285.
Komai, Y. & Ushiki, T. (1991). *Invest. Ophthalmol. Vis. Sci.* **32**, 2244–2258.
Linsenmayer, T. F., Fitch, J. M. & Birk, D. E. (1990). *Ann. N.Y. Acad. Sci.* **580**, 143–160.
Linsenmayer, T. F., Fitch, J. M., Gordon, M. K., Cai, C. X., Igoe, F., Marchant, J. K. & Birk, D. E. (1998). *Prog. Retin. Eye Res.* **17**, 231–265.
Liu, C. Y., Birk, D. E., Hassell, J. R., Kane, B. & Kao, W. W.-Y. (2003). *J. Biol. Chem.* **278**, 21672–21677.
Maurice, D. M. (1957). *J. Physiol.* (*London*), **186**, 263–286.

Meek, K. M., Elliott, G. F., Sayers, Z., Whitburn, S. B. & Koch, M. H. J. (1981). *J. Mol. Biol.* **149**, 477–488.
Meek, K. M., Fullwood, N. J., Cooke, P. H., Elliott, G. F., Maurice, D. M., Quantock, A. J., Wall, R. S. & Worthington, C. R. (1991). *Biophys. J.* **60**, 467–474.
Meek, K. M. & Quantock, A. J. (2001). *Prog. Retin. Eye Res.* **20**, 95–137.
Meek, K. M., Quantock, A. J., Boote, C., Liu, C. Y. & Kao, W. W.-Y. (2003). *Matrix Biol.* **22**, 467–475.
Meek, K. M., Leonard, D. W., Connon, C. J., Dennis, S. & Khan, S. (2003). *Eye*, **17**, 927–936.
Muller, L. J., Pels, E. & Vrensen, G. F. J. M. (2001). *Br. J. Ophthalmol.* **85**, 437–443.
Polack, F. M. (1961). *Am. J. Ophthalmol.* **51**, 179–184.
Quantock, A. J., Kinoshita, S., Capel, M. C. & Schanzlin, D. J. (1998). *Biophys. J.* **74**, 995–998.
Quantock, A. J., Meek, K. M., Brittain, P., Ridgway, A. E. A. & Thonar, E. J.-M. A. (1991). *Tissue Cell*, **23**, 593–606.
Quantock, A. J., Meek, K. M. & Chakravarti, S. (2001). *Invest. Ophthalmol. Vis. Sci.* **42**, 1750–1756.
Radner, W., Zehetmayer, M., Aufreiter, R. & Mallinger, R. (1998). *Cornea*, **17**, 537–543.
Sayers, Z., Whitburn, S. B., Koch, M. H. J., Meek, K. M. & Elliott, G. F. (1982). *J. Mol. Biol.* **160**, 593–607.
Siegler, V. & Quantock, A. J. (2002). *Exp. Eye Res.* **74**, 427–431.
Song, J., Lee, Y.-G., Houston, J., Petrol, W. M., Chakravarti, S., Cavanagh, H. D. & Jester, J. V. (2003). *Invest. Ophthalmol. Vis. Sci.* **44**, 548–557.
Young, R. D., Tudor, D., Hayes, A. J., Kerr, B., Hayashida, Y., Nishida, K., Meek, K. M., Caterson, B. & Quantock, A. J. (2005). *Invest. Ophthalmol. Vis. Sci.* **46**, 1973–1978.